



# Determination of the Binding Situation of Pyridine in Xylan Sulfates by Means of Detailed NMR Studies

Lars Gabriel, Wolfgang Günther, Friederike Pielenz, and Thomas Heinze\*

Xylan sulfate is an important drug to treat interstitial cystitis. Production of the drug by sulfation of the polysaccharide with a sulfating agent like chlorosulfuric acid and pyridine–SO<sub>3</sub> complex in pyridine may lead to products containing pyridine-based impurities. Xylan sulfate containing nitrogen is investigated by different NMR measurements in order to clarify the binding situation of pyridine. The detailed NMR studies allow the conclusion that the pyridine-based impurities are covalently bonded to the reducing end group. Furthermore, the NMR spectroscopic investigation indicates that the side reactions occur at shorter polymer chains only.

heterogeneous conditions yields a product that exhibits no pyridinium impurities.<sup>[5]</sup> Thus, this indirect approach is an additional hint that a reaction of the reducing end groups is the reason for the introduction of pyridine moieties into XS. To get an unambiguous direct proof and clarify the binding situation of pyridine in XS, detailed NMR spectroscopic studies including diffusion ordered spectroscopy (DOSY) of XS obtained by heterogeneous synthesis were carried out.

## 1. Introduction

Sulfated polysaccharides are important compounds in living organism that exhibit a number of biological functions.<sup>[1]</sup> Semi-synthetic polysaccharide sulfates possess also promising biological properties and may be adjusted to the function in question by controlling the degree of sulfation and the functionalization pattern.<sup>[2]</sup> The commercially produced pentosan polysulfate (PPS) obtained from the hemicellulose xylan is used in various pharmaceutical products.<sup>[3]</sup> For the synthesis of PPS, a heterogeneous procedure using ClSO<sub>3</sub>H and pyridine is applied. The SO<sub>3</sub>-pyridine complex as reactive intermediate and pyridinium hydrochloride are formed during the course of synthesis.<sup>[4]</sup> The structural purity of semisynthetic polysaccharide sulfates including PPS is an important prerequisite for pharmaceutical applications. It was described that pyridine molecules may be linked to the polymer in addition to the desired sulfate groups.<sup>[4]</sup> That pyridinium sulfate does not exist was concluded from UV spectroscopic studies and extraction of an aqueous solution of xylan sulfate (XS) at pH value of 10 with chloroform. It was assumed that pyridine is covalently linked to the reducing end group. This hypothesis is supported by the fact that a treatment of the xylan with NaBH<sub>4</sub> and subsequent sulfation under

## 2. Results and Discussion

Sulfation of polysaccharides is a common tool to generate water-soluble and bioactive polysaccharide derivatives.<sup>[2,6–8]</sup> In this context, xylan sulfate (XS) commercially called pentosan polysulfate (PPS) is of particular interest. Unfortunately, it was revealed that XS obtained by heterogeneous sulfation in pyridine, which is the process commercially applied by various producers worldwide, may contain nitrogen-containing impurities resulting from side reactions with pyridine (**Figure 1**). These impurities may yield undesired biological activities.

For these studies, sulfation of xylan was performed in pyridine applying ClSO<sub>3</sub>H as sulfating agent comparable to the commercial processes.<sup>[5]</sup> Two different XS samples with a degree of substitution (DS) of 1.49 (**XS-1**) and 1.74 (**XS-2**) were prepared. The XS samples were characterized by <sup>1</sup>H- and <sup>13</sup>C-NMR spectroscopy. The typical signals could be assigned to the corresponding H- and C atoms (**Figure 2**).

In the <sup>1</sup>H-NMR spectrum of XS, various signals appeared at chemical shifts above 8 ppm, which are not compatible with the structure of the sulfated polysaccharide. Typical spectra are shown in **Figure 2**. These signals appear in the spectra of both samples (**XS-1** and **XS-2**) although they slightly differ regarding to their intensity and line width (**Figure 3**). Due to the use of pyridine in the heterogeneous synthesis, most of the downfield-signals could be correlated to pyridinium ions. Further signals appear at a chemical shift around 9.3 ppm as singlets that could not be assigned based on the NMR spectra measured up to now.

In a further set of detailed NMR spectroscopic experiments, pyridinium hydrochloride was added to the **XS-1** samples and the <sup>1</sup>H-NMR spectrum was acquired again. The typical spectrum of **XS-1** with additional pyridinium hydrochloride is shown in **Figure 3b**. The signals of the pyridinium hydrochloride appear slightly high-field shifted compared to the signals of the impurities discussed above. This result indicates that the impurities do not result from protonated pyridine ions. It turned out that the signals of the impurities exhibit a similar intensity ratio of 2:1:2 compared

L. Gabriel, Dr. W. Günther, F. Pielenz, Prof. T. Heinze  
Institute of Organic Chemistry and Macromolecular Chemistry  
Centre of Excellence for Polysaccharide Research  
Friedrich Schiller University of Jena  
Humboldtstraße 10, D-07743 Jena, Germany  
E-mail: thomas.heinze@uni-jena.de

The ORCID identification number(s) for the author(s) of this article can be found under <https://doi.org/10.1002/macp.201900327>.

© 2019 The Authors. Published by WILEY-VCH Verlag GmbH & Co. KGaA, Weinheim. This is an open access article under the terms of the Creative Commons Attribution License, which permits use, distribution and reproduction in any medium, provided the original work is properly cited.

DOI: 10.1002/macp.201900327

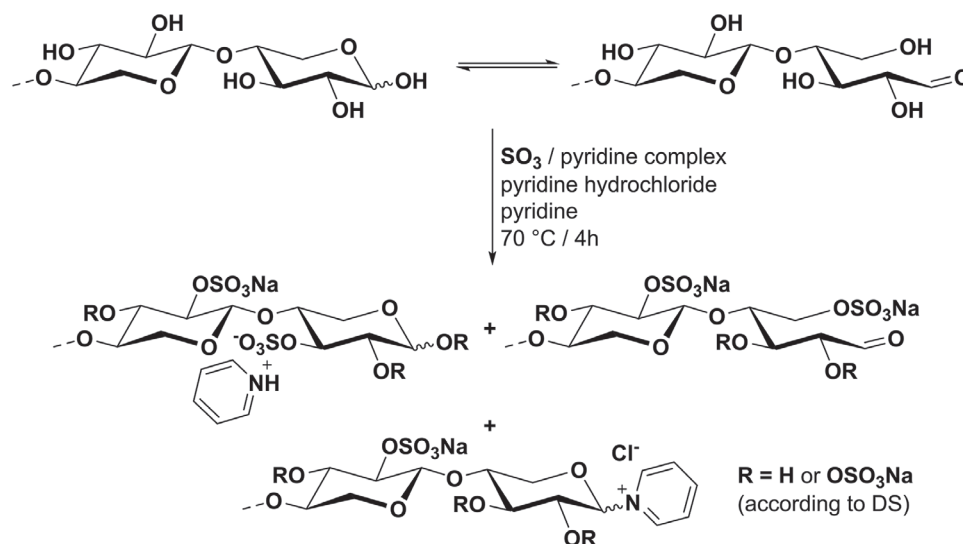


**Figure 1.** Reaction scheme of the sulfation of xylan with  $\text{SO}_3$ /pyridine complex in pyridine showing possible reaction products.

to the pyridinium hydrochloride (Figure 3a,b). Therefore, the impurity may be a pyridinium moiety that might be bonded to the polymer chain via the nitrogen atom. The same results were found for **XS-2**. Further investigations were performed with sample **XS-2** due to the comparably lower line-width of the signals although sample **XS-2** contains about 5% of pyridinium ions.

Previously, it could be shown that a treatment with  $\text{NaBH}_4$  leads to a reduced xylan. Using this reduced xylan a XS (heterogeneous synthesis in pyridine) could be synthesized that possess no signals in the  $^1\text{H-NMR}$  spectra above 8 ppm.<sup>[5]</sup> By the treatment with  $\text{NaBH}_4$ , the terminal  $\alpha$ - or  $\beta$ -xylopyranose unit is converted into xylitol, which is linked in position 2 to the polymer chain. Therefore, the non-protonated pyridinium impurity has to be covalently linked to the reducing end group. To get a closer look, a rotational nuclear overhauser effect spectroscopy (ROESY) measurement with selective excitation of the 2,6-protons at 9.2 ppm was performed (Figure 4).

In the ROESY spectrum, the signals at 6.02 and 6.33 ppm are interesting. The proton at 6.33 ppm appears as doublet with a coupling constant of 1.4 Hz. The signal at 6.02 ppm is a doublet with a coupling constant of 6.8 Hz. A proton shift range restricted HSQC shows that the proton at 6.02 ppm belongs to a carbon with a shift of 93 ppm and the hydrogen at 6.33 ppm is bonded to a carbon with a shift of 89.5 ppm (1, Supporting Information). These coupling- and shift data indicate that they belong to the anomeric positions of sugar molecules (6.02/93 ppm for the beta- and 6.33/89.5 ppm for the alpha anomer). It should be noted that the two anomers must not be isomers, they could have different degrees of sulfation.

For the identification of the remaining protons of the terminal xylopyranose units, total correlation spectroscopy (TOCSY) measurements with selective excitation and various mixing times were performed. For the alpha form of the xylopyranose units, these experiments failed, because

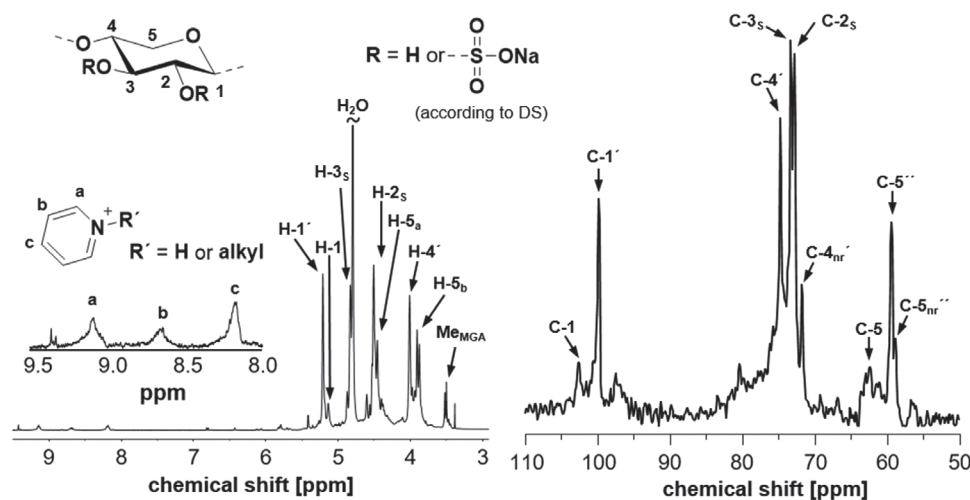


**Figure 2.**  $^1\text{H}$ - (left) and  $^{13}\text{C}$ -NMR spectra (right) of xylan sulfate (**XS-2**) with a degree of substitution of 1.74, recorded in  $\text{D}_2\text{O}$ . Indications: s: sulfation in the corresponding position, ' : sulfation in adjacent position, '' : influenced by sulfation in position 2 and/or 3, MGA – 4-O-methylglucuronic acid.

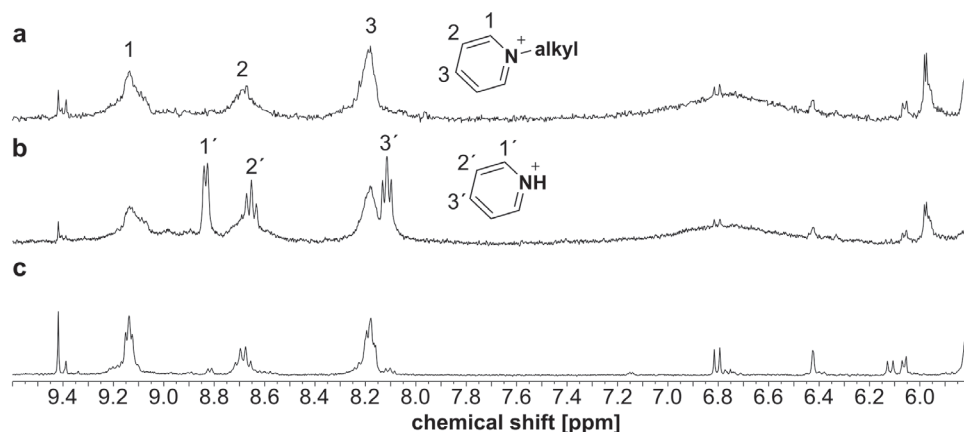


**Figure 3.** Area of low-field proton signals in the a)  $^1\text{H-NMR}$  spectra of xylan sulfate XS-1, b) XS-1 with pyridinium hydrochloride added, and c) XS-2.

of the weak coupling between H-1 and H-2. However, a successful TOCSY measurement of the beta anomer was possible (Figure 5). The excitation was performed using a selective pulse on the anomeric proton at 6.02 ppm. Using a mixing time of 25 ms, the H-2 appeared at 4.69 ppm (triplet). Applying a mixing time of 80 ms, the remaining protons could be identified (H-3 as triplet at 4.83 ppm, H-4 at 4.36 ppm, two protons bonded to C-5 at 4.58 and 4.05 ppm, for the protons in position 4 and 5 the multiplicity could not be specified).

Another interesting fact is that the signal intensities in the pyridine spin system exhibit the usual deviations in the range of some percent. Setting the integral values for the 2,6-protons of the pyridinium at a value of 2, the summarized intensities of the anomeric protons just reached a value of 0.63 (Figure 6). Due to this result, the main structure of the pyridine-substituted end groups includes only around 63% of the intensity expected. The exact structure of these main components remains unknown because of missing information about the sulfation pattern. A closer look at the signal of the 2,6 protons reveals a lot of small signals on both sides of the main signals. These small signals were caused by the 2,6 protons of alpha and

beta anomer not sulfated and with different degrees of substitution (mono- and disulfated). The chemical shift of the anomeric protons of these different forms could be slightly different for each structure. Thus, the signal-to-noise ratios are too small for a detection of these protons.

The previously mentioned singlets at a chemical shift of 9.3 ppm (see Figure 3) are correlated to a signal with chemical shift of 190.5 ppm in the HSQC spectrum indicating that they result from the aldehyde moieties of the reducing end groups of the polymer. Thus, the aldehyde and a primary hydroxyl group at position 5 are formed due to the oxo-cyclo-tautomerism. The hydroxyl group at C-5 formed by the ring opening could also be sulfated during the lifetime of the oxo-form. This sulfation reaction prevents the back reaction caused by oxo-cyclo-tautomerism into the hemiacetal. As a result, an enrichment of the aldehyde moiety is possible. The aldehyde formation is another path of modification of the reducing end group and competes with the reaction with pyridine. In the  $^1\text{H-NMR}$  spectrum, the signals of the aldehyde appear as sharp singlets and not as doublets as expected. The reason may be a proton-deuterium-exchange in position 2. Both CH-acidity and keto-enol tautomerism can

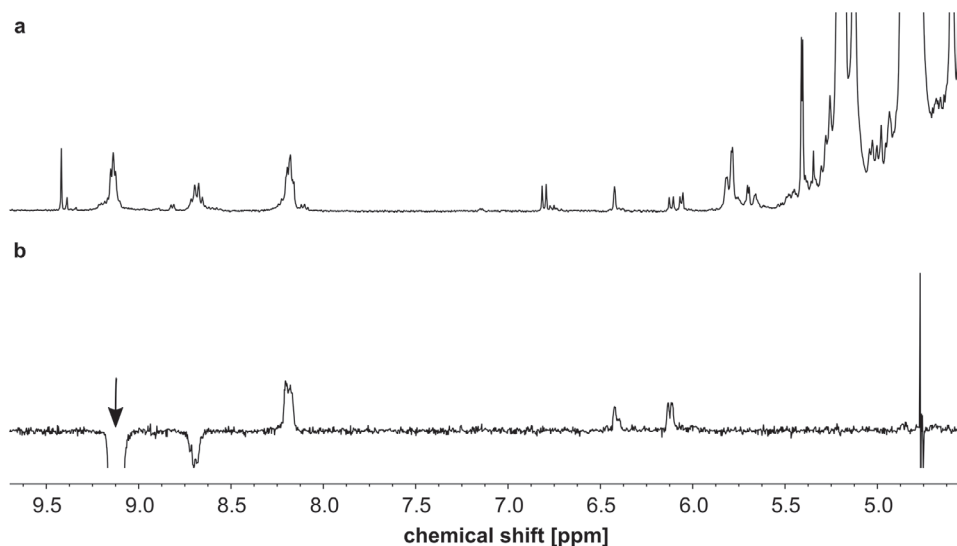


**Figure 4.** a)  $^1\text{H-NMR}$  spectrum of xylan sulfate XS-2 and b) selective ROESY-NMR spectrum of XS-2 after selective excitation of the signal at 9.14 ppm ( $\rightarrow$ ).

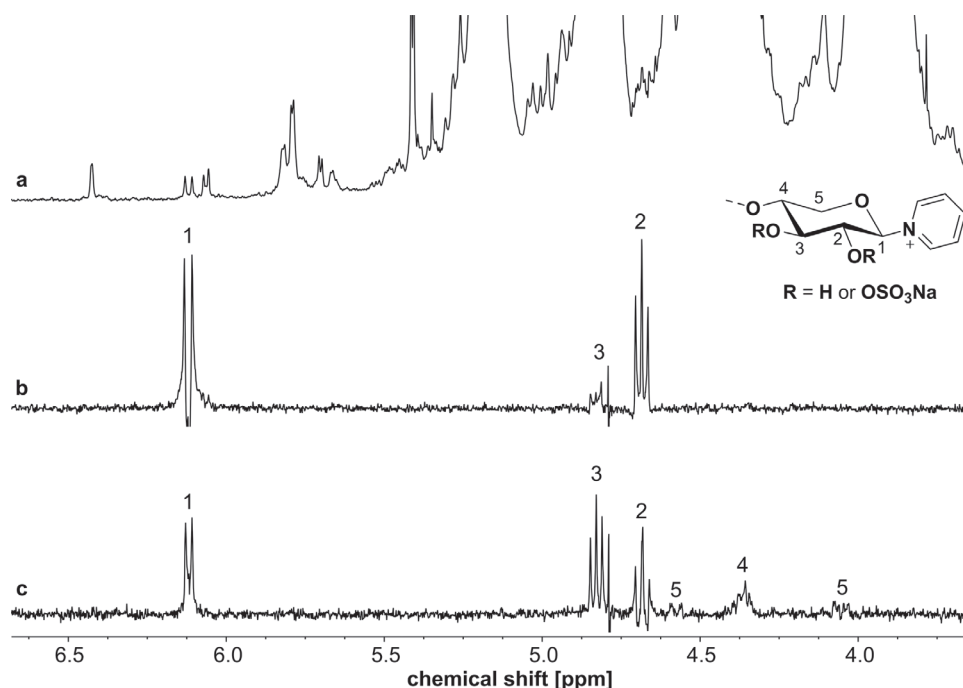


**Figure 5.** a)  $^1\text{H}$ -NMR spectrum of xylan sulfate XS-2 in comparison to the corresponding selective TOCSY-NMR spectra recorded with different mixing times of b) 25 ms and c) 80 ms.

be responsible for this process and the remaining coupling between the aldehyde proton and the deuterium atom at C-2 could be very small.

Moreover, DOSY measurements can give additional valuable information. The diffusion coefficient is dependent on the concentration and the molecular size and consequently on the number average of the molecular weight ( $M_n$ ). For our investigations, the concentration dependence of the diffusion coefficient was not relevant, because we want to get a qualitative statement of the diffusion coefficient only. In **Figure 7**, the DOSY spectrum of XS-2 is shown. The values of the diffusion coefficients of the xylan signals are in the range of  $1 \times 10^{-10} \text{ m}^2 \text{ s}^{-1}$ . The values for aldehyde and pyridinium appear significantly higher at  $D = 1.318 \cdot 10^{-10} \text{ m}^2 \text{ s}^{-1}$  (for comparison, a free pyridinium ion appears at a value of  $5.011 \cdot 10^{-10} \text{ m}^2 \text{ s}^{-1}$  and water appears at  $D = 1.584 \cdot 10^{-9} \text{ m}^2 \text{ s}^{-1}$ ). This finding indicates that the aldehyde and the pyridinium are linked to macromolecules with the low  $M_n$ , which belongs to the normal  $M$  distribution ( $\bar{D}$ ). Obviously, the

reducing end groups of the larger macromolecules cannot react in the sulfation reaction under these conditions.

More information could be obtained from the Stejskal-Tanner plot.<sup>[9–11]</sup> In a simple form, the plot is based on the following equation (further information given in Supporting Information):

$$\ln\left(\frac{I(q)}{I_0}\right) = -Dq \quad (1)$$

$$\text{with } q = \gamma^2 g^2 \delta^2 \left( \Delta - \frac{\delta}{3} \right)$$

$q$  is a product of natural constants, experimental diffusion parameters, and a variable space-dependent magnetic field gradient,  $D$  is the diffusion coefficient,  $I(q)$  is the integral of a NMR signal depending on  $q$  and  $I_0$  is the intensity at  $q = 0$ . In a Stejskal-Tanner plot with logarithmic intensity scale, the monoexponential decay of a defined molecule appears as a linear slope while a polymers multiexponential decay will be visible

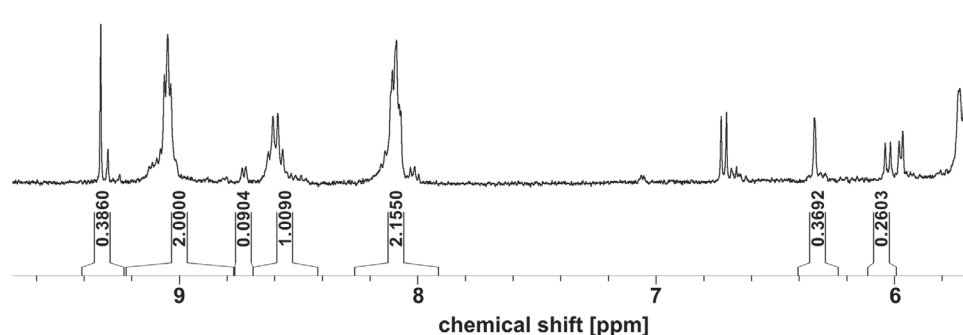


**Figure 6.** Integral intensity in the  $^1\text{H}$ -NMR-spectra of the impurity of XS-2.

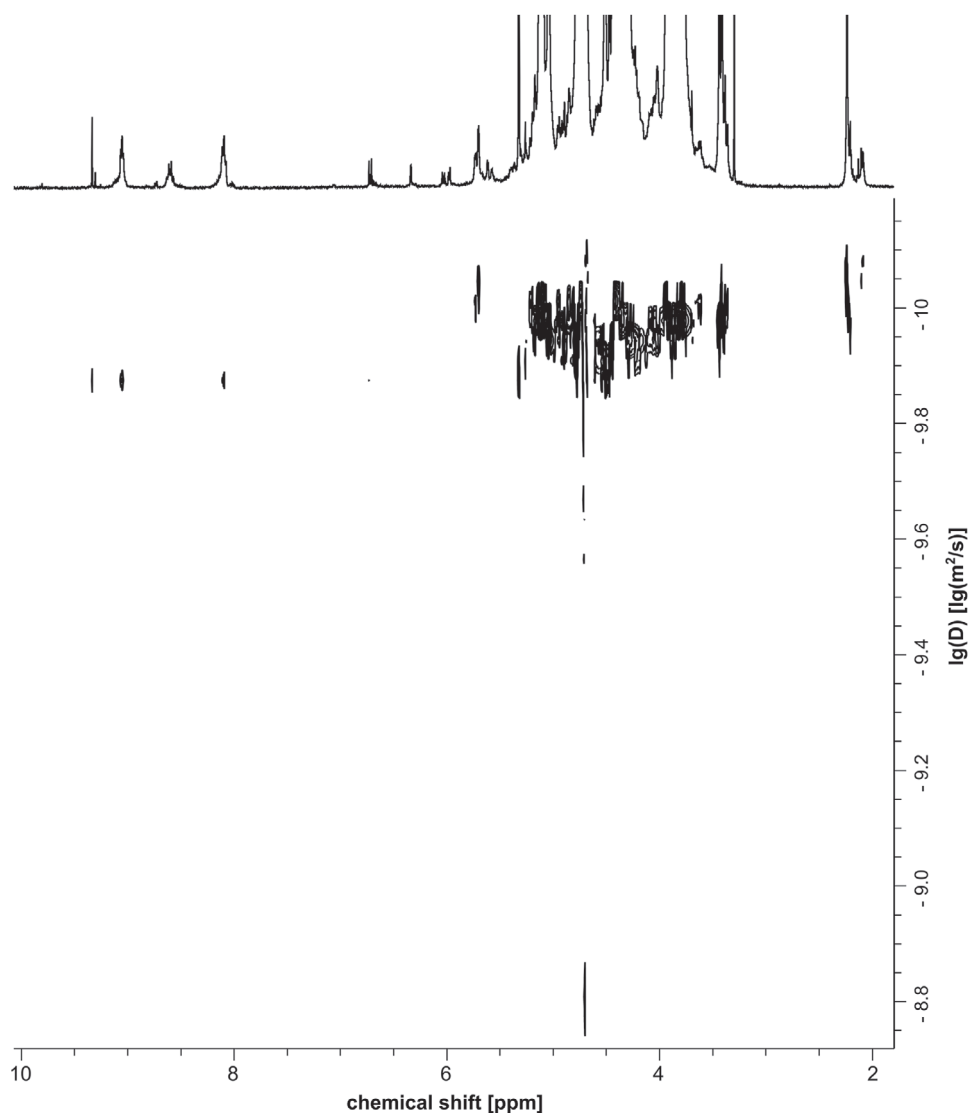
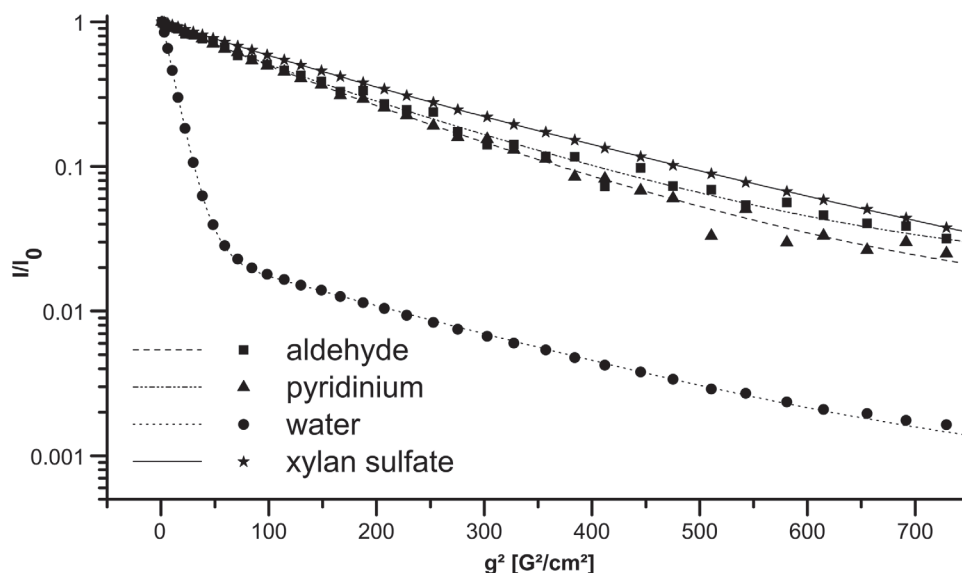


Figure 7. DOSY-NMR spectrum of xylan sulfate (XS-2).

as curved function depending on the shape and width of  $\mathcal{D}$ . In Figure 8 the Stejskal–Tanner plots are shown for the signals of aldehyde, pyridinium (2,6-protons), XS (near H-4 and H-5b), and water. The water included in the sample results from the NMR solvent containing traces of water, however, mainly from water included in the polymer sample. As expected, XS has the lowest diffusion coefficients, that is, XS is the most slowly moving component. For small  $q$ -values, water, as the smallest molecule, has the steepest negative slope, but with increasing the  $q$ -values, the diffusion properties of water approach those of XS. Due to a small overlapping of the water signal with the signal of H-3<sub>s</sub>, this second diffusion behavior of the water signal results partly from the influence of the polymer peak, but also from the solvation shell of XS. Furthermore, aldehyde and pyridinium are diffusing with the same velocity, but they exhibit significantly higher diffusion coefficients compared to XS. From the spin-echo-decay of the XS and the water, a distribution function of the diffusion coefficient can be calculated

using the inversion of the Laplace transformation (Figure 9). In Figure 9 the distribution of the diffusion coefficients of XS and water are shown.<sup>[12,13]</sup> The left part of the diffusion coefficient distribution of the water signal is partly caused by the already mentioned overlapping of the water signal and the signal of H-3<sub>s</sub>. Nevertheless, based on the results, it is revealed that two types of water are present and that the distribution of hydration-linked water (the small left peak) has a great similarity with the XS distribution. Unfortunately, there is no simple way to get  $\mathcal{D}$  from the distribution of diffusion coefficients.

In principle, the integrals of the <sup>1</sup>H-NMR spectra could be used for the determination of  $M_n$  of polymers. In case of XS, there are three different end groups present, namely the aldehyde resulting from the sulfation in position 5, the pyridinium moiety, and the unmodified one. The integrals of the aldehyde and pyridinium moieties are definable from the proton spectrum. The signals resulting from the unmodified xylopyranose end group are not available, because of the similar chemical



**Figure 8.** Stejskal–Tanner plot of spin-echo-decay of the components contained in XS-2. The intensity is plotted versus the strength of the field gradient ( $g$ ). To show the course of the diffusion coefficients, a biexponential fit-function according to the Stejskal–Tanner equation was used.

shift compared to the polymer backbone. Using an independent experimental method for the determination of  $M_n$ , the percentage ratio of the different end groups is accessible. Size exclusion chromatography (SEC) of XS-2 (DS 1.74) exhibits a degree of polymerization (DP) of 16. From the analysis of the DOSY measurements, it is known that the larger polymer chains do not react with the pyridine. Therefore, the sum of the integral intensities of the aldehyde and pyridinium moieties gave a kind of upper limit of the degree of polymerization ( $DP_{UL}$ ) according to the following equation:

$$DP_{UL} = \frac{I_{Bulk}}{I_{Ald} + I_{Pyr}} \quad (2)$$

$I_{Bulk}$  is the halved integral of signals relating to proton H-4 and H-5<sub>b</sub> around 4 ppm.  $I_{Ald}$  and  $I_{Pyr}$  represent the integral intensities of the aldehyde modified in position 5 and of one proton of the pyridinium moiety. According to Equation (2), the  $DP_{UL}$  exhibits a value of 38. The real DP of the polymer could be calculated as follows:

$$DP = \frac{I_{Bulk}}{I_{Ald} + I_{Pyr} + I_{Xyl}} \quad (3)$$

If one or more protons of the xylopyranose end group have a chemical shift in the same range of  $I_{bulk}$ , the value of  $I_{bulk}$  could be slightly increased (in case of all six protons of the end

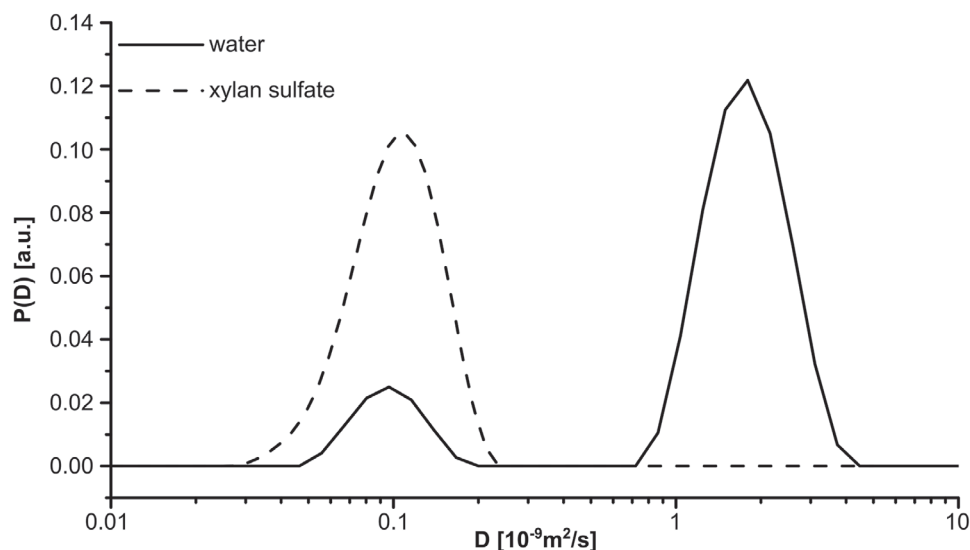


**Figure 9.** Plot of the diffusion coefficient distribution of the components contained in sample XS-2.



group this range is max. 10%). However, from Equations (2) and (3), the experimentally inaccessible value of  $I_{\text{xyl}}$  is accessible according to the following equation:

$$I_{\text{xyl}} = \frac{I_{\text{Bulk}}}{\text{DP}} - \frac{I_{\text{Bulk}}}{\text{DP}_{\text{UL}}} \quad (4)$$

The calculation exhibits that 55% of the polymer chains carries a pyridinium-modified end group. 22% exhibit an aldehyde resulting from a sulfation of position 5 and 23% of the polymer chains remain unmodified. This result indicates that the main part of the XS forms the pyridinium salt at the end group under the reaction conditions applied.

### 3. Conclusions

For the first time an analytical proof for the binding situation of pyridine is given that is usually found in xylan sulfates obtained by a heterogeneous sulfation of xylan in pyridine with chlorosulfonic acid ( $\text{SO}_3$ -pyridine complex). The pyridine signals belong to pyridinium ions that are linked to a carbon. Various NMR spectroscopic methods including selective ROESY, TOCSY, and DOSY measurements verify that the pyridinium is covalently linked to the reducing end groups of the xylan sulfate. Calculation of the ratio of the different end groups exhibit that the main part of the polymer chains are modified by a pyridinium moiety. Regarding the use of xylan sulfate in pharmaceuticals, structurally pure xylan sulfate is highly desired that may be produced by excluding pyridine applying a homogeneous reaction in solvents like *N,N*-dimethyl acetamide/LiCl, for example.

### 4. Experimental Section

**Materials:** All solvents and reagents were obtained from Sigma Aldrich and used without further purification. Deuterium oxide (99.9%) for the NMR measurements were purchased from Deutero GmbH (Kastellaun, Germany). Xylan from beech wood was provided by bene pharmaChem GmbH & Co. KG (Geretsried, Germany).

**Methods and Measurements:** Xylan sulfate (XS) was synthesized and characterized as described in previous work.<sup>[5]</sup> All NMR measurements of xylan derivatives were recorded at 24 °C in deuterium oxide with a Bruker Avance III 400 MHz spectrometer.  $^1\text{H}$ -,  $^{13}\text{C}$ -, and TOCSY experiments were performed with a sample concentration of 60 mg mL<sup>-1</sup>. For the DOSY-NMR measurements, a concentration of 40 mg mL<sup>-1</sup> was used; a diffusion time ( $\Delta$ ) of 119.9 ms and gradient pulse duration ( $\delta$ ) of 8 ms were used. For the DOSY experiments, magnetic field gradient strength ( $g$ ) was varied in the range from 0.01 to 0.48 T m<sup>-1</sup>. Size exclusion chromatography (SEC) was performed on a JASCO system (isocratic pump PU-980, RI-930 refractive index detector) with a Novema 3000 and a Novema 300 column in series. A 0.1 M  $\text{NaNO}_3$  aqueous solution with 0.05 wt%  $\text{NaN}_3$  was used as eluent (70 °C, flow rate: 0.5 mL min<sup>-1</sup>) and pullulan as calibration standard (342–710 000 g mol<sup>-1</sup>).

### Supporting Information

Supporting Information is available from the Wiley Online Library or from the author.

### Acknowledgements

The authors would like to thank Annett Pfeifer (Institute of Organic Chemistry and Macromolecular Chemistry, Centre of Excellence for Polysaccharide Research, Friedrich-Schiller-University of Jena) for support in the preparation of xylan sulfate. Furthermore, the authors would like to acknowledge the NMR platform at the Friedrich-Schiller-University Jena for support in the NMR spectroscopy. Moreover, the authors thank Petrik Galvosas (Victoria University of Wellington, Wellington, New Zealand) for providing the software for generating the distribution of the diffusion coefficients.

### Conflict of Interest

The authors declare no conflict of interest.

### Keywords

diffusion ordered spectroscopy (DOSY), NMR spectroscopy, pyridine, total correlation spectroscopy (TOCSY), xylan sulfate

Received: July 31, 2019  
Revised: September 11, 2019  
Published online: October 10, 2019

- [1] L. Fransson, in *The Polysaccharides* (Ed: G. O. Aspinall), Academic Press, New York **1985**, pp. 3–337.
- [2] T. Heinze, S. Daus, M. Gericke, T. Liebert, in *Polysaccharides: Development, Properties and Applications* (Ed: A. Tiwari), Nova Science Publishers, New York **2010**, pp. 213–259.
- [3] A. Ebringerová, Z. Hromádková, *Biotechnol. Genet. Eng. Rev.* **1999**, 66, 325.
- [4] L. Ahrgren, A. de Belder, T. Mälson, *Carbohydr. Polym.* **1991**, 16, 211.
- [5] A. Pfeifer, T. Heinze, *Carbohydr. Polym.* **2019**, 206, 65.
- [6] B. Vega, K. Petzold, P. Fardim, T. Heinze, *Carbohydr. Polym.* **2012**, 89, 768.
- [7] L. J. Herrero, S.-S. Foo, K.-C. Sheng, W. Chen, M. R. Forwood, R. Bucala, S. Mahalingam, *J. Virol.* **2015**, 89, 8063.
- [8] S. Daus, K. Petzold-Welcke, M. Kötteritzsch, A. Baumgaertel, U. S. Schubert, T. Heinze, *Macromol. Mater. Eng.* **2011**, 296, 551.
- [9] D. Sinnaeve, *Concepts Magn. Reson. Part A* **2012**, 40A, 39.
- [10] M. S. Kaucher, Y.-F. Lam, S. Pieraccini, G. Gottarelli, J. T. Davis, *Chem. - Eur. J.* **2005**, 11, 164.
- [11] E. O. Stejskal, J. E. Tanner, *J. Chem. Phys.* **1965**, 42, 288.
- [12] P. Galvosas, P. T. Callaghan, *C. R. Phys.* **2010**, 11, 172.
- [13] X. Guo, E. Laryea, M. Wilhelm, B. Luy, H. Nirschl, G. Guthausen, *Macromol. Chem. Phys.* **2017**, 218, 1600440.